



How alanine catalyzes melanoidin formation and dehydration during synthesis from glucose

Ghassan Faisal Mohsin¹ · Franz-Josef Schmitt² · Clemens Kanzler³ · Azaldeen Kazal Alzubaidi⁴ · Andrea Hornemann⁵

Received: 28 October 2021 / Revised: 16 February 2022 / Accepted: 18 February 2022 / Published online: 15 March 2022
© The Author(s) 2022

Abstract

The chemical composition of melanoidins formed from glucose (Glc) and alanine (Ala) in different molar ratios was investigated using UV/Vis, FTIR, EPR spectroscopy and elemental analysis (EA). Melanoidin samples were prepared at varying molar ratios of Glc and Ala ranging from 10:1 to 1:10 (Glc:Ala). Reaction systems containing a higher molar ratio of Ala show higher melanoidin yields and higher UV/Vis absorbance. This indicates that an excess of Ala facilitates the formation of larger π -electron systems and catalyzes the melanoidin formation. EPR spectroscopy showed more radicals in Ala enriched samples. The EA data suggest that during the formation of melanoidin from Glc and Ala higher amounts of amino acid support dehydration of the reaction products. On the basis of our data, we postulate the structures of products and intermediates for the reaction at different Glc/Ala ratios. PCA of the FTIR spectra allows to separate different melanoidin samples formed at varying molar ratios indicating their different molecular compositions.

Keywords Melanoidin · D-Glucose · L-Alanine · Principal component analysis · FTIR · Dehydration

Abbreviations

| | |
|--------|--|
| Ala | L-Alanine |
| EPR | Electron paramagnetic resonance |
| FTIR | Fourier transformation infrared (spectroscopy) |
| Glc | D-Glucose |
| HMW | High molecular weight |
| NMR | Nuclear magnetic resonance |
| PCA | Principal component analysis |
| UV/Vis | Ultraviolet/visible (spectroscopy) |

Introduction

The Maillard reaction (MR) plays a key role in producing taste, flavor and color of food products [1–4]. It is initialized by the condensation of reducing sugars and amino compounds such as amino acids or proteins and a subsequent conversion resulting in Amadori rearrangement products (ARP). In the following intermediate stage of the MR, the ARP might undergo a variety of parallel and consecutive reactions. In the course of these reactions, the amino acid residues play a key role in catalyzed dehydration reactions, usually in which hundreds of MR products containing C=C and C=O double bonds are generated which determine the UV/Vis absorption and therefore the color of the resulting reaction products. In the final step of the MR high-molecular-weight polymers, the so-called melanoidins are formed, causing the visible browning of foods during heat treatment. Melanoidins can be isolated from various foods such as coffee, beer, bread crust, malt, and dried fruits [5, 6].

Relevant reactions occurring during the intermediate stage are the formation of deoxyosones, most notably 3-deoxyglucosone (3-DG) by dehydration as well as fragmentation reactions leading to short-chain acids, carbonyls or 1,2-dicarbonyl compounds such as formic acid, acetic acid, acetaldehyde or methylglyoxal (MGO). MGO and

✉ Franz-Josef Schmitt
franz-josef.schmitt@physik.uni-halle.de

¹ Ministry of Education, Department of Vocational Education in Maysan, General Directorate Vocational Education, Maysan 62001, Iraq

² Martin-Luther-Universität Halle-Wittenberg, Institute of Physics, von-Danckelmann-Platz 3, 06120 Halle, Germany

³ Department of Food Chemistry and Analysis, Technische Universität Berlin, Institute of Food Technology and Food Chemistry, Gustav-Meyer-Allee 25, 13355 Berlin, Germany

⁴ College of Agriculture, University of Misan, Al-amarah 62001, Iraq

⁵ Physikalisch-Technische Bundesanstalt, Abbestr. 2-12, 10587 Berlin, Germany

3-DG might undergo the Strecker degradation with amino acids resulting in Strecker aldehydes and α -amino ketones. Model studies employing MGO and Ala showed that these products are integrated into melanoidin backbones [7].

Parallel to the MR the amino acids may form dipeptides, cyclopeptides or other still unknown linkages without involvement of the carbohydrate [8, 9]. In the absence of amino acids, carbohydrates undergo caramelization reactions and eventually form colorants based on transglycosidation reactions [10] or based on polymerization of the dehydration product 3-DG [11, 12]. Because of the multitude of involved reaction products that might be integrated in the melanoidin backbone in the course of the MR studies that help to cluster and classify possible end products based on different reaction conditions, it is necessary to investigate the composition of melanoidins and to better understand their role in food quality, for example, the flavors, colors and anti-oxidant properties [13–15].

Our previous investigations [16–18] followed this approach by varying temperature, reactants and reaction conditions of the MR and analyzed the resulting melanoidins. Mohsin et al. [17] successfully confirmed the structure of melanoidins produced from D-glucose (Glc) and L-alanine (Ala) at various temperatures by means of FTIR as proposed by Cämmerer and Kroh [19]. It was found that important functional groups of the respective reactants and the intermediates during the reaction, such as carboxyl (COOH) and carbonyl (C=O) or double-bond carbon (C=C) and imine (C=N), respectively, are involved in the structure of the polymers. The structure proposed by Cämmerer and Kroh [19] also fits the molecular composition analyzed by elemental analysis, for instance by [17, 20, 21]. Our studies included multivariate statistics techniques such as principal component analysis (PCA) showing that the differences in the FTIR spectra are determined by the ratio of characteristic vibrational modes between 1030 cm^{-1} and 1150 cm^{-1} assigned to C–O and the stretching vibrations of C=O at $1745\text{--}1610\text{ cm}^{-1}$. Moreover, the FTIR fingerprints are suitable to cluster and identify different melanoidins with respect to their structural composition [18]. Besides FTIR, a variety of analytical methods can be used to characterize food or model melanoidins. For example, free radicals in polymers are well known and can be characterized by EPR [22]. The color of melanoidins caused by delocalized π -electron systems is studied by UV/Vis spectroscopy [23, 24]. Elemental analysis of carbon, hydrogen, and nitrogen quantifies the amount of amino acid found in the reaction products.

The present study is focused on the influence of the molar ratio of the reactants on the structure and the formation of melanoidins, because our previous investigations indicated different reaction mechanisms depending on the availability of the carbohydrates and amino compounds as well as possible catalytic effects of alanine [16]. For this reason,

melanoidins were prepared from Glc and Ala mixed in molar ratios from 10:1 to 1:10. The samples were analyzed by means of FTIR, EPR, UV/Vis spectroscopy and EA. Glc and Ala were selected to prepare the model melanoidins in this study, because they are ubiquitously found in foods and represent most typical reactants in the MR. The reaction conditions are based on baking or roasting conditions as typical process steps of food production.

Materials and methods

Chemicals and reagents

D-Glucose ($\geq 99.5\%$) was obtained from Carl Roth (Karlsruhe, Germany), L-alanine was obtained from Fluka (Steinheim, Germany), and potassium bromide was obtained from Sigma-Aldrich (Steinheim, Germany). The dialysis tubing was made from cellulose with a molecular weight cutoff (MWCO) of ca. 12,000–14,000 Da and ordered from Carl Roth (Karlsruhe, Germany).

Preparation of model melanoidins

Melanoidins were prepared according to [17]. Glc and Ala were mixed in different molar ratios (10:1, 2:1, 1:1, 1:2, 1:5 and 1:10) and heated in a flat sheet for 10 min at $160\text{ }^{\circ}\text{C}$.

Clean-up of raw melanoidins

The dialysis was performed according to Mohsin et al. [17]. The dry crude reaction products were ground in a mortar before being dialyzed. The dialysis tubing (Spectrum Por, Carl Roth, Germany) was composed of cellulose with a molecular weight cutoff (MWCO) around 12,000–14,000 Da and pore size of 1.5–3.0 nm (thickness: 23 nm and width: 33 mm). Batch dialysis was achieved by dissolving 2.5 g of the reaction products in 150 mL of distilled water and putting it into the dialysis tube. The distilled water was exchanged every 10 h, resulting in a total dialysis time of ca. 136 h.

FTIR spectroscopy: instrumentation and data acquisition

Melanoidin samples were measured as previously described [17]. FTIR measurements were recorded at the IR beamline ‘IRMA’ of the Metrology Light Source (MLS) storage ring of PTB. Experiments were done with a Vertex-80v FTIR spectrometer coupled to an IR microscope Hyperion 3000 (Bruker Optics GmbH, Germany) equipped with a 128^2 pixels FPA (Focal Plane Array) detector (pixel size $\sim 3\text{ }\mu\text{m}$ at magnification $15\times$). Mid-IR spectroscopy (MIR) from

1900 cm^{-1} to 900 cm^{-1} was obtained in transmission geometry by co-adding 128 scans at 4 cm^{-1} spectral resolution. Background scans were collected before sample measurements from a KBr sample pellet and subtracted from the respective sample spectrum. For data representation, 100 randomly picked spectra were chosen and shown with standard deviation as envelope.

EPR spectroscopy

EPR measurements were carried out on a MiniScope MS 100 spectrometer (Magnetech, Berlin, Germany) in accordance with Mohsin et al. [17]. The following acquisition parameters were used: magnetic flux density 3390 G, modulation amplitude 1500 mG, sweep time 30 s, sweep width 150 G. Microwave power was set to 15.8 mW (8 dB). A glass rod was used to compress 2.5–3.5 mg of sample into an NMR tube. Three measurements were taken for each sample and the obtained signal strength was normalized to the total sample weight with standard deviation.

UV/Vis spectroscopy

Melanoidins were measured as previously described [17] using a UV/Vis spectrometer (Specord 200 Plus, Analytik Jena, Jena, Germany). A melanoidin sample of 0.5 mg was dissolved in 1 mL distilled water. The wavelength range from 300 to 800 nm was measured against a blank, containing distilled water only.

Elemental analysis

A Flash EA 1112 Organic Elemental Analyzer was used to conduct the elemental analysis of carbon, hydrogen, and nitrogen (Thermo Fisher Scientific, Dreieich, Germany). Since only Glc and Ala were used to produce melanoidin, the amount of oxygen could be determined by subtracting the sum of the quantified elements from 100%. Melanoidin in the range of 1–3 mg was used for each analysis. Duplicate measurements were taken for each sample (Table 2).

Principal component analysis (PCA)

Principal component analysis was performed in the fingerprint region between 1900 cm^{-1} –900 cm^{-1} with MatlabR2012a[®] (The MathWorks, Inc), applying the Toolboxes “stats” and “PLS_Toolbox_795”. For calculation of principal components (PCs), 100 spectra per sample of six different samples were used, forming a PCA matrix of 600 spectra (311,400 datapoints) in total. This matrix comprised the spectral window, the absorbance (z) values stacked over the x – y dimension. Analysis was performed

in the spectral window between 1900 cm^{-1} and 900 cm^{-1} . Data pre-processing entailed mean centering, a baseline correction (weighted least squares), Savitzky–Golay algorithm for smoothing (polynom third order, window length: 15 cm^{-1}) and vector normalization. Data were illustrated by PC scatter plots from PC1 to PC4 including their corresponding loading spectra (Fig. S-2).

Results and discussion

FTIR spectra of melanoidins formed from Glc and Ala in various molar ratios

Figure 1 shows the FTIR absorbance in the range of 1900–900 cm^{-1} of melanoidins prepared in molar ratios of 10:1, 2:1, 1:1, 1:2, 1:5 and 1:10 from Glc and Ala. Attention was given to this spectral window, because it covers most of the spectral variance.

The comparison of these spectra to spectra of heated Glc and heated Ala from our previous study shows distinctive differences [17]. Consequently, pure Ala or Glc as well as possible polymers formed from these during heat treatment were efficiently removed by dialysis and not integrated into the melanoidins to a relevant extent.

An overview on all characteristic bands of the prepared samples as shown in Fig. 1 is given in Table 1. All bands appear broadened due to a structural inhomogeneity of the samples, caused by the variety of different colorants formed by the MR. Among the most characteristic IR signals were the bands at 1745 cm^{-1} resulting from stretching vibrations of carbonyl (C=O) or carboxyl (COOH) groups [25] and 1640 cm^{-1} (with a shoulder at 1610 cm^{-1}) attributed to the stretching vibration in carboxylate (COO⁻) [26, 27]. In contrast, C–O single bond bending vibrations occur in the 1080–1035 cm^{-1} range and both areas (1745–1610 cm^{-1} and 1080–1035 cm^{-1}) were shown to be crucial for the classification of different molecular MR compositions [16, 18].

Figure 1 and Table 1 show how the bands at 1745–1610 cm^{-1} rise with increasing amino acid concentration compared to 1080 cm^{-1} and 1035 cm^{-1} . It is related to stretching vibrations of C=O, C=N, and C=C, or Amide I (see Table 1, Fig. S-1) [16, 18]. C–O single bonds contributing to the bands at 1080–1035 cm^{-1} are replaced by carbonyl (C=O) and carbon double (C=C) bonds when the content of alanine rises during the reaction.

EPR spectra of melanoidins based on Glc and Ala at various molar ratios

With EPR spectroscopy, unpaired electrons and consequently organic radicals can be studied [36]. Radicals formed during the MR might be transferred to the conjugated

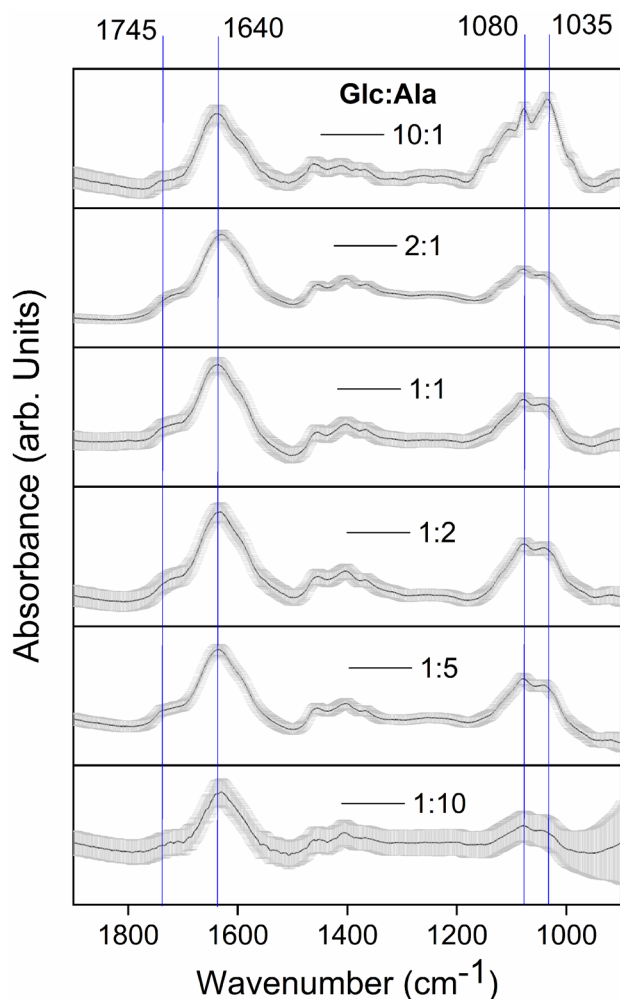


Fig. 1 Infrared spectra in the spectral window of 1900–900 cm^{-1} of melanoidins prepared from Glc and Ala at 160 °C for 10 min at various molar ratios. The solid lines represent average spectra and the gray envelopes indicate standard deviations ($n=100$)

melanoidin skeletons. These radicals are identified using EPR spectroscopy. According to the EPR results, the radical character of melanoidins prepared at varying molar ratios from Glc and Ala increases with the amount of amino acid used for preparation of the corresponding melanoidin sample (Fig. 2). This observation indicates that melanoidins prepared with an excess of Ala contain more substructures that are able to stabilize radicals. Most likely, a larger conjugated double-bond system is responsible. This interpretation is supported by the higher UV/Vis absorbance, the IR spectra and the elemental analysis of the corresponding samples, which also suggest more C=C and C=O double bonds.

UV/Vis spectroscopy

UV/Vis spectroscopy is commonly used as semi-quantitative measure for the melanoidin content in aqueous extracts of

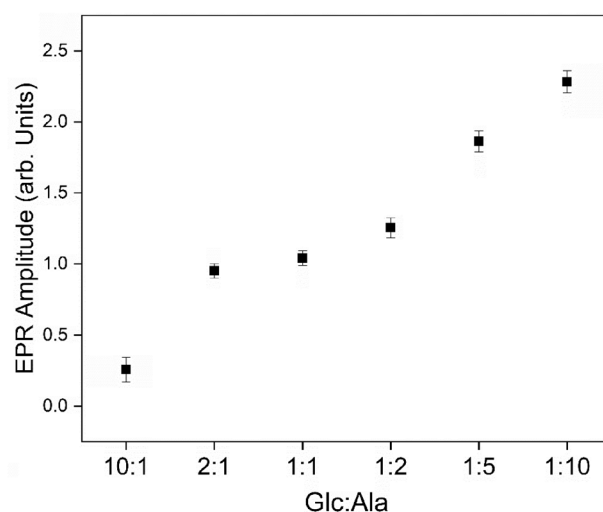


Fig. 2 EPR signal intensity obtained from melanoidin samples prepared from Glc and Ala at different molar ratios. The relative signal strength per mass unit is shown with standard deviation ($n=3$)

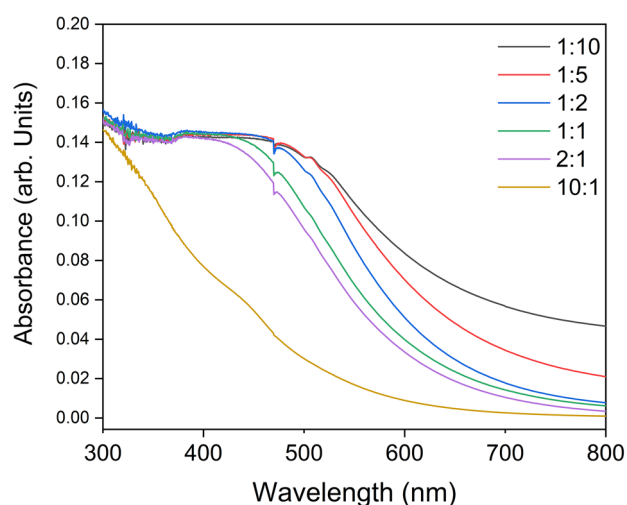


Fig. 3 UV/Vis absorbance spectra of melanoidins formed at different molar ratios of Glc and Ala at 160 °C

MR mixtures. As seen in Fig. 3 the melanoidin samples prepared in this study show a continuous increase in absorption with higher content of Ala used for preparation (see Fig. 3) including a significant shift of the absorbance band at a ratio of 10:1 (Glc:Ala) toward shorter wavelengths, indicating less chromophores and smaller π -electron systems than melanoidins prepared from an excess of Ala. The amount of conjugated double bonds is one of the most important factors influencing the UV/Vis absorbance by a molecule. Renn and Sathe [23] concluded that an excess of amino acid was more effective in increasing the browning rate than the excess of glucose under the same conditions. Similar results

were found by Shen et al. [24]. Combining these findings with the semi-quantitative FTIR analysis and results of the EA allows for a possible reaction scheme that might suggest new intermediate structures appearing during the dehydration reaction (see Fig. 4).

Elemental analysis and yield of the high-molecular-weight MR products

Table 2 shows the carbon, hydrogen, nitrogen and oxygen contents of melanoidins formed from Glc and Ala at molar ratios of 5:1, 2:1, 1:1, 1:2 and 1:5. When Glc and Ala react at an equimolar ratio (1:1), the nitrogen content of the formed melanoidin (%N=3.315) suggests that per mole amino acid two moles of carbohydrate are integrated into the melanoidin backbone. If the initial molar ratio of 1:1 would be adopted in the melanoidin the nitrogen content would have to be above 5%. At a molar ratio of 2:1 (Glc:Ala) during the formation the nitrogen content of the resulting melanoidin is nearly identical to the equimolar preparation and does not significantly change when the ratio of Glc is further increased (See Table 2). This indicates that an excess of carbohydrate does not alter the general formation mechanism. Consequently, at all molar ratios of 1:1, 2:1 and 5:1 (Glc:Ala), the skeleton of melanoidin is considered to be composed of two sugar moieties per amino nitrogen.

On the other hand, an excess of amino acid (1:2, Glc:Ala) increases the nitrogen content of the melanoidin by 20%. This could be caused by integration of more amino acid per mole of carbohydrate in the backbone. However, this trend quickly saturates and does not show significant change when Glc:Ala is offered at a molar ratio of 1:5 (See Table 2).

Therefore, it can be concluded that this increase of the N/C ratio does not necessarily account for a general change in ratio of carbohydrate to amino acid in the backbone of the melanoidin. In addition, as seen by UV/Vis spectroscopy, the melanoidin samples prepared with an excess of amino acid show a considerably higher absorbance indicating that an excess of Ala facilitates the formation of larger π -electron systems and larger amounts of sp^2 hybridized carbon (see Fig. 3). In the context of the results of the elemental analysis this indicates that a higher nitrogen content in melanoidins is connected to the formation of more chromophores and/or of chromophores with a higher molar extinction [16]. The decrease in hydrogen and oxygen indicates the elimination of water that would result in the formation of double-bond and conjugated double-bond systems.

The question arises, if a rising content of Ala leads to stronger catalytic efficiency of Ala and if it is catalyzing both, formation of high-molecular-weight MR products and dehydration of polymers during or after their formation. To answer this question, the yield of high-molecular-weight MR products after dialysis was compared with the theoretically expected yield as displayed in Table 3.

2.5 g of the MR reaction products was dissolved in 150 mL of distilled water and put into dialysis tubes. After dialysis, the melanoidins were freeze-dried and weighted. The yield continuously rises with Ala content from $0.4 \pm 0.04\%$ (Glc:Ala 10:1) to $1.1 \pm 0.04\%$ (Glc:Ala 1:10) with a highest amount of 27 ± 1.0 mg purified melanoidin for melanoidins at a ratio Glc:Ala, 1:10 after dialysis of 2.5 g of reaction products.

From this analysis, two important findings are derived: 1) high-molecular-weight MR products typically yield less than

Table 1 Vibrational modes and their tentative assignments to functional groups found in sugar- and amino acid-enriched melanoidins which appear broadened (br), strong (s), medium (m) or weak (w)

| Wavenumber (cm ⁻¹) | Modes | Sugar-enriched melanoidin (Glc:Ala 10:1) | Amino acid-enriched melanoidin (Glc:Ala 1:10) | References |
|--------------------------------|---|--|---|---------------------|
| 3500–3000 | $\nu(\text{O-H})$ | br | br | [16–18, 28–30] |
| 3300 | $\nu(\text{NH})$, amide A | br, overlap | br, overlap | [31, 32] |
| 3100 | $\nu(\text{NH})$, amide B | w, overlap | w, overlap | [25] |
| 2930 | $\nu(\text{CH}_3)$ | w | w | [30, 33, 34] |
| 2860 | $\nu(\text{CH}_2)$ | w | w | [33, 34] |
| 1745 | $\nu(\text{COOH})$ or $\nu(\text{C=O})$, | w | w | [16–18, 25] |
| 1640 | $\nu(\text{COO}^-)$ | s | s | [16–18, 26, 27] |
| 1630–1610 | $\nu(\text{COO}^-)$, $\nu(\text{C=O})$ or $\nu(\text{C=C})$, $\nu(\text{C=N})$, amide I | m | m | [18, 29, 30, 35] |
| 1455 | $\nu(\text{C-N})$, $\delta(\text{N-H})$, amide II | w | w | [16–18] |
| 1400 | $\nu(\text{C-N})$, $\delta(\text{N-H})$, $\delta(\text{CH}_3)$, $\delta(\text{CH}_2)$, amide II | w | w | [16–18, 34] |
| 1365 | $\nu(\text{C-N})$ or $\delta(\text{O-H})$, $\delta(\text{CH}_3)$, amide II | w | w | [16–18, 34] |
| 1220 | amide III or $\nu(\text{C-O})$ | w | w | [16–18, 34] |
| 1080–1035 | $\delta(\text{C-O})$ or $\delta(\text{C-H})$ | s | w | [16–18, 29, 30, 34] |
| 920 | $\nu(\text{C-C})$ in the carbohydrate structure, $\delta(\text{C-H})$ | w | w | [16–18, 29, 34] |

1% of the overall reaction products and 2) the MR product yield with high molecular weight steadily rises with rising content of Ala indicating that the formation of melanoidins itself is catalyzed by Ala.

Based on the results of the EA, melanoidins formed from Glc and Ala generally contain two carbohydrate moieties per molecule of Ala and an excess of Ala facilitates dehydration reactions; however, the latter effect is limited at molar ratios above 1:2 (Glc:Ala). The overall yield of high-molecular-weight melanoidins is further increased at ratios of 1:5 and 1:10 indicating that an excess of Ala catalyzes the formation of these MR colorants.

Structural conclusions

Derived from these empirical findings, a reaction pathway for the formation of melanoidins containing two carbohydrate backbones per mole of amino acid is postulated in Fig. 4. The condensation of Glc and Ala and the subsequent rearrangement result in the formation of the ARP (initial stage of the MR) [37]. Elimination of water at C3 yields the most prevalent 1,2-dicarbonyl compound of the MR 3-DG in form of its imine. Finally, hydrolysis of the amino acid results in free 3-DG. Both of the latter compounds form polymeric structures by aldol condensation reactions and nucleophilic substitution reactions.

The resulting melanoidin structure [A] is based on a postulation of Cämmerer & Kroh [19] as well as our previous publication [17]. Subsequent dehydration would result in the formation of C=C and C=O double bonds and more potent chromophores such as structure [B] emerge. In addition, intramolecular cyclization reactions might occur and lead to the formation of furan-like substructures like [C] comparable to structures identified by Bruhns et al. [12] and Kanzler et al. [7] by means of high-resolution mass spectrometry. The elemental composition of the proposals [A] and [B] are close to the results of the elemental analysis of the melanoidin sample formed from Glc and Ala at a ratio of 1:1 and 1:2 (Glc:Ala), respectively. Though the amount of incorporated amino acid does not effectively change from [B] to [C], the elimination of water shifts the theoretical nitrogen content from 3.88 to 4.08%. It can be concluded that in this instance, the role of the amino acid is to catalyze dehydration reactions and promote the general browning reaction as described by Kaufmann et al. [38], rather than being a reactant that is integrated into the melanoidin skeleton at excess.

Naturally, in melanoidin samples a variety of different structures and substructures is to be expected [19, 38–40], and therefore in all melanoidin samples in this study, substructures such as [A], [B] and [C] will dominate based on our finding, but also related substructures will be present. Apart from 3-DG, other 1,2-dicarbonyl compounds such

as glucosone, 1-deoxyosone and MGO or carbonyl compounds such as acetaldehyde, furfural and hydroxymethylfurfural could undergo comparable reactions. Kanzler et al. [7] could show that melanoidin backbones are indeed composed of a variety of structurally related MR products including products typically formed in the Strecker degradation, namely Strecker aldehydes and α -aminoketones. In addition, products of carbohydrate fragmentation reactions further diversify the structure of melanoidins. This variety of the involved reactants explains the slight differences between the theoretical elemental composition of the proposed products (Fig. 4) and the experimentally determined elemental composition (Table 2). The samples in our study are always complex mixtures of different melanoidins in which the proposed substructures are prevalent.

Depending on the content of free amino acids during the formation of the respective melanoidin, the degree of dehydration of the polymers may vary. A higher content of amino acids facilitates more dehydration reactions and consequently the structures [B] and [C] will dominate and shift the elemental composition toward the measured values of the melanoidin prepared from Glc and Ala at a ratio of 1:2.

Principal component analysis of sugar- and amino acid-enriched melanoidins

Principal component analysis (PCA) is one of the multivariate statistical methods, which can advantageously be used for the characterization and identification of various melanoidins [18]. The present results show that structurally different melanoidins that are formed at different molar ratios of Glc:Ala can be distinguished by means of PCA, conducted in the spectral window between 1900 cm^{-1} and 900 cm^{-1} which is abundant in spectral features. This region, including the stretching vibrations of C–O at 1080–1035 cm^{-1} and C=O (COOH) at 1745–1640 cm^{-1} , will be the focus of this section. Figure 5 displays the PC score plots from PC1 to PC4 which capture 92.4% of the total variance (See Table S-1). With an increasing amount of alanine (Glc:Ala 1:2, 1:5 and 1:10, respectively), these melanoidin compositions are allocated opposite to the sugar-enriched samples (Glc:Ala 2:1 and 10:1) in the scores diagram of PC1 versus PC2. They are negatively correlated with respect to PC2 which is mainly composed of vibrational peaks in the range between 1700 and 1600 cm^{-1} , i.e., stretching vibrations of double bonds of carbon (C=C) and carbonyl (C=O) (Fig. S-2). This is a clear evidence that a differentiation and separation among both types of melanoidin compositions (excess of amino acid versus excess of sugar during preparation) is possible with respect to the C=C and C=O content, balanced by the 1:1 Glc–Ala composition (green cluster), which can be found perfectly allocated in between both types. Similar motifs are observed in the PC2 versus PC3, and PC2 versus

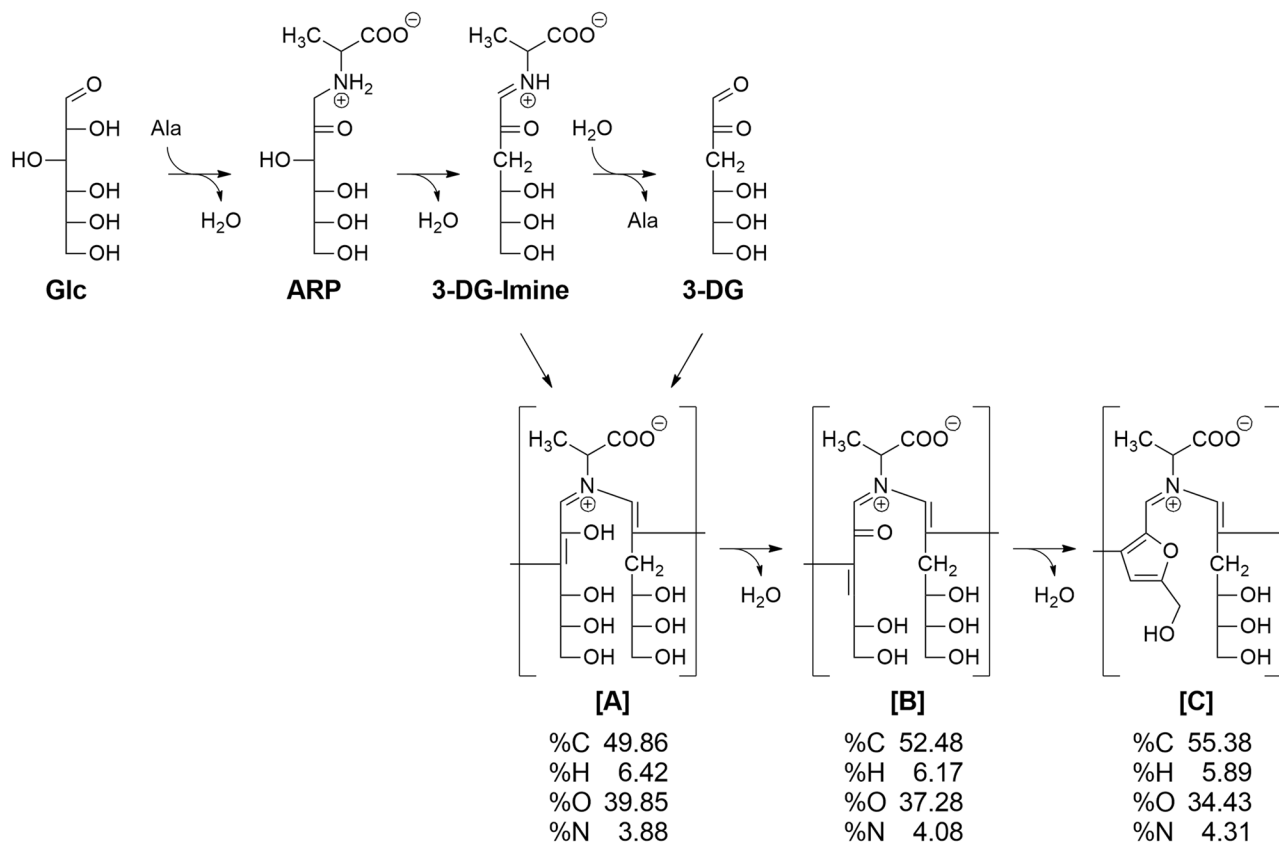


Fig. 4 Proposed pathway for the formation of melanoidins containing two carbohydrate backbones per mole of amino acid (**A**). Subsequent amino-catalyzed dehydration reactions yield the structures (**B** and **C**)

Table 2 Elemental composition of melanoidins formed from Glc:Ala at 5:1, 2:1, 1:1, 1:2 and 1:5 at 160 °C for 10 min

| Molar ratio Glc:Ala | %C | %H | %O | %N | H/C | O/C | N/C |
|------------------------|--------|-------|--------|-------|-------|-------|-------|
| 5:1 | 49.34 | 6.08 | 41.10 | 3.48 | 0.123 | 0.833 | 0.071 |
| 2:1 | 49.420 | 6.215 | 40.860 | 3.505 | 0.126 | 0.827 | 0.071 |
| 1:1 | 48.855 | 6.285 | 41.545 | 3.315 | 0.129 | 0.85 | 0.068 |
| 1:2 | 50.550 | 6.255 | 38.905 | 4.290 | 0.124 | 0.77 | 0.085 |
| 1:5 | 50.46 | 6.30 | 38.89 | 4.35 | 0.125 | 0.77 | 0.086 |

Every sample was measured twice

PC4 score plots. The spectral contributions being responsible for these observations can be found in the corresponding loadings spectra (Fig. S-2 and Table S-1). To conclude, the separability of these different compositions is mainly caused by the spectral features of carboxyl or carbonyl groups in the 1745–1640 cm⁻¹ window, which dominate in PC1 and PC2. Also, the C–O stretching vibrations found between 1080 and 1035 cm⁻¹ are partially represented by PC1, but with a smaller contribution.

Conclusion

In our previous studies, melanoidins were synthesized from glucose and alanine at different temperatures [17] or from different carbohydrate compounds [18]. These studies showed that higher UV/Vis absorption of melanoidins is correlated with more C=C, C=O and C=N groups which are crucial for the formation of chromophores. The FTIR spectra (Fig. 1) for various melanoidins formed from different ratios of Glc:Ala indicated that an excess of Ala during melanoidin formation induces the formation of these groups

Table 3 Yield of high-molecular-weight melanoidins formed from Glc:Ala at 10:1, 5:1, 2:1, 1:1, 1:2 and 1:5 and 1:10 at 160 °C for 10 min after dialysis of 2.5 g MR product before dialysis

| Molar ratio Glc:Ala | Glc (mass) | Ala (mass) | MR product after dialysis | Experimental yield |
|------------------------|------------|------------|------------------------------|-----------------------|
| 10:1 | 180 g | 9 g | 10 ± 1.0 mg | 0.4 ± 0.04% |
| 5:1 | 180 g | 18 g | 12 ± 1.0 mg | 0.5 ± 0.04% |
| 2:1 | 180 g | 45 g | 13 ± 1.0 mg | 0.5 ± 0.04% |
| 1:1 | 180 g | 90 g | 18 ± 1.0 mg | 0.7 ± 0.04% |
| 1:2 | 90 g | 90 g | 20 ± 1.0 mg | 0.8 ± 0.04% |
| 1:5 | 36 g | 90 g | 22 ± 1.0 mg | 0.9 ± 0.04% |
| 1:10 | 18 g | 90 g | 27 ± 1.0 mg | 1.1 ± 0.04% |

and corresponding chromophores as well as higher content of free radicals (Figs. 2 and 3). Elemental analysis and FTIR spectra show dehydration and in consequence formation of C=C and C=O double bonds resulting in more potent chromophores that occur with higher content of Ala during melanoidin formation. Cyclization and further dehydration

reactions might even lead to the formation of furan-like substructures (Fig. 4).

Considering the dual role of Ala as catalyst and reactant, the combined findings of UV–Vis (Fig. 3), EA (Table 2) and yield (Table 3) show that Ala mainly accelerates the reaction and functions as a catalyst for dehydration and formation of melanoidin up to ratios of Glc:Ala of 1:2 but primarily as catalyst for the overall melanoidin formation at ratios of Glc:Ala above 1:2. It can practically be ruled out that additional glucose moieties are incorporated into the polymer backbone after formation of polymeric MR products, because an excess of Glc during melanoidin formation does not affect the N/C ration significantly. On the other hand, an excess of Ala shows that the role of the amino acid lies in catalyzing dehydration reactions and promoting the general browning reaction as described by Kaufmann et al. [38] for the MR in general. In addition, the present approach shows that even if the FTIR spectra of the different preparations are quite similar, each preparation delivers melanoidins with a specific spectral FTIR pattern. Consequently, dominating

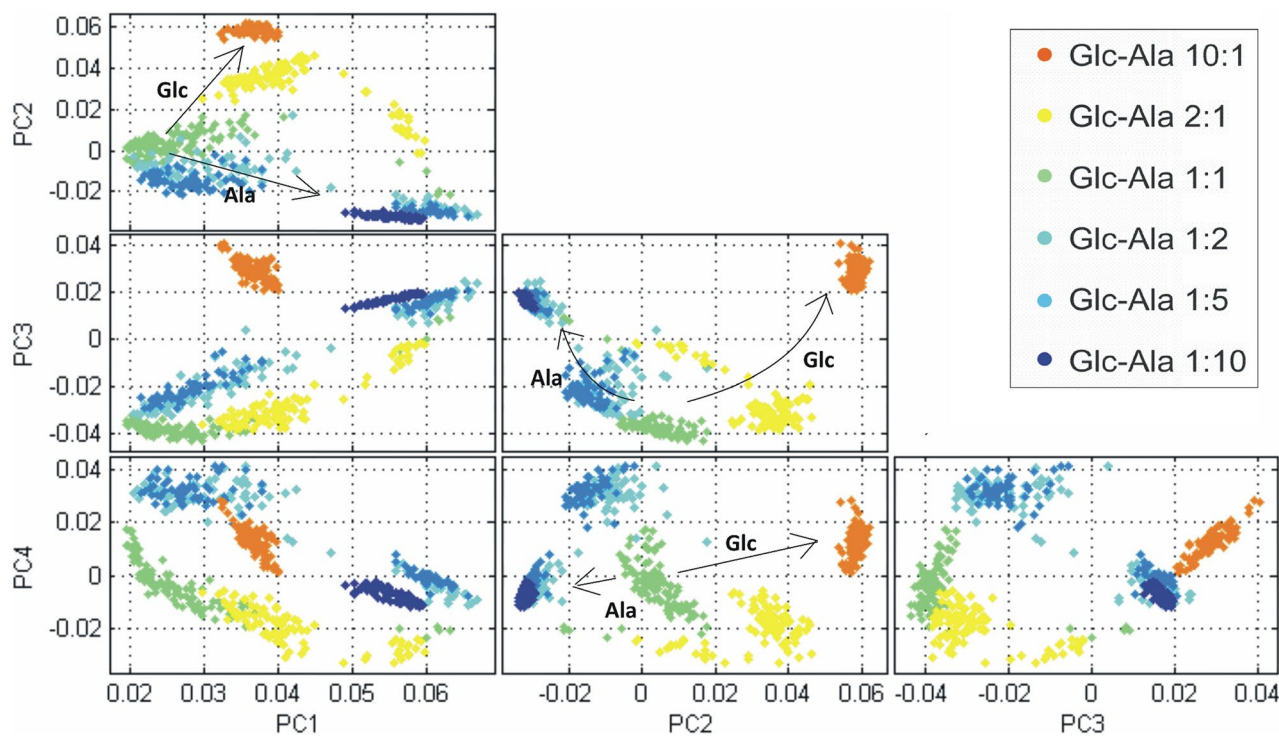


Fig. 5 PCA analysis of the melanoidins formed at different molar ratios

structures and substructures can be distinguished by PCA depending on the ratio of sugar and amino acid (Fig. 5).

Supplementary Information The online version contains supplementary material available at <https://doi.org/10.1007/s00217-022-03989-x>.

Funding Open Access funding enabled and organized by Projekt DEAL.

Declarations

Conflict of interest The authors declare no conflicts of interest.

Compliance with ethics requirements This study does not contain any studies with human participants or animals performed by any of the authors.

Open Access This article is licensed under a Creative Commons Attribution 4.0 International License, which permits use, sharing, adaptation, distribution and reproduction in any medium or format, as long as you give appropriate credit to the original author(s) and the source, provide a link to the Creative Commons licence, and indicate if changes were made. The images or other third party material in this article are included in the article's Creative Commons licence, unless indicated otherwise in a credit line to the material. If material is not included in the article's Creative Commons licence and your intended use is not permitted by statutory regulation or exceeds the permitted use, you will need to obtain permission directly from the copyright holder. To view a copy of this licence, visit <http://creativecommons.org/licenses/by/4.0/>.

References

- Ames JM (1990) Control of the Maillard reaction in food systems. *Trends Food Sci Tech* 1:150–154. [https://doi.org/10.1016/0924-2244\(90\)90113-D](https://doi.org/10.1016/0924-2244(90)90113-D)
- Cossu A, Posadino AM, Giordo R, Emanuelli C, Sanguinetti AM, Piscopo A, Poiana M, Capobianco G, Piga A, Pintus G (2012) Apricot melanoidins prevent oxidative endothelial cell death by counteracting mitochondrial oxidation and membrane depolarization. *PLoS ONE* 7(11):e48817. <https://doi.org/10.1371/journal.pone.0048817>
- Echavarría AP, Pagán J, Ibarz A (2013) Antioxidant activity of the melanoidin fractions formed from D-glucose and D-fructose with L-asparagine in the maillard reaction. *Sci Agropecu* 4(1):45–54. <https://doi.org/10.17268/sci.agropecu.2013.01.05>
- Huang M, Zhang X, Karangwa E (2015) Comparison sensory characteristic, non-volatile compounds, volatile compounds and antioxidant activity of MRPs by novel gradient temperature-elevating and traditional isothermal methods. *J Food Sci Technol* 52(2):858–866. <https://doi.org/10.1007/s13197-013-1083-y>
- Echavarría AP, Pagán J, Ibarz A (2012) Melanoidins formed by maillard reaction in food and their biological activity. *Food Eng Rev* 4:203–223. <https://doi.org/10.1007/s12393-012-9057-9>
- Zhang H, Zhang H, Troise AD, Fogliano V (2019) Melanoidins from coffee, cocoa, and bread are able to scavenge α -dicarbonyl compounds under simulated physiological conditions. *J Agric Food Chem* 67(39):10921–10929. <https://doi.org/10.1021/acs.jafc.9b03744>
- Kanzler C, Wustrack F, Rohn S (2021) High-resolution mass spectrometry analysis of melanoidins and their precursors formed in a model study of the maillard reaction of methylglyoxal with L-alanine or L-lysine. *J Agric Food Chem* 69(40):11960–11970. <https://doi.org/10.1021/acs.jafc.1c04594>
- Liang Z, Li L, Qi H, Wan L, Cai P, Xu Z, Li B (2016) Formation of peptide bound pyrrolidine in the maillard model systems with different Lys-containing dipeptides and tripeptides. *Molecules* 21(4):463. <https://doi.org/10.3390/molecules21040463>
- Zou T, Kang L, Yang C, Song H, Liu Y (2019) Flavour precursor peptide from an enzymatic beef hydrolysate Maillard reaction-II: Mechanism of the synthesis of flavour compounds from a sulphur-containing peptide through a Maillard reaction. *LWT* 110:8–18. <https://doi.org/10.1016/j.lwt.2019.04.022>
- Golon A, Kuhnert N (2012) Unraveling the chemical composition of caramels. *J Agric Food Chem* 60(12):3266–3274. <https://doi.org/10.1021/jf204807z>
- Cämmerer B, Jalyschko W, Kroh LW (2002) Intact carbohydrate structures as part of the melanoidin skeleton. *J Agric Food Chem* 50:2083–2087
- Bruhns P, Kanzler C, Degenhardt AG, Koch TJ, Kroh LW (2019) Basic Structure of melanoidins formed in the Maillard reaction of 3-deoxyglucosone and γ -aminobutyric acid. *J Agric Food Chem* 67(18):5197–5203. <https://doi.org/10.1021/acs.jafc.9b00202>
- Liu HM, Han YF, Wang NN, Zheng YZ, Wang XD (2020) Formation and antioxidant activity of Maillard reaction products derived from different sugar-amino acid aqueous model systems of sesame roasting. *J Oleo Sci* 69(4):391–401. <https://doi.org/10.5650/jos.ess19336>
- Li Y-L, Zhu Y-Z, Zheng P-H, Qu Z-Y, Zhang H, Hou W, Piao X-M, Wang Y-P (2021) Potentially Harmful Maillard Reaction Products in Food and Herb Medicines. *J Food Qual ID* 1798936:11. <https://doi.org/10.1155/2021/1798936>
- Ni ZJ, Liu X, Xia B, Hu LT, Thakur K, Wei ZJ (2021) Effects of sugars on the flavor and antioxidant properties of the Maillard reaction products of camellia seed meals. *Food Chem X* 11:100127. <https://doi.org/10.1016/j.fochx.2021.100127>
- Mohsin GF, Schmitt FJ, Kanzler C, Epping JD, Bührke D, Hornemann A (2020) Melanoidin formed from fructosylalanine contains more alanine than melanoidin formed from d-glucose with L-alanine. *Food Chem* 305:125459. <https://doi.org/10.1016/j.foodchem.2019.125459>
- Mohsin GF, Schmitt FJ, Kanzler C, Dirk Epping J, Flemig S, Hornemann A (2018) Structural characterization of melanoidin formed from d-glucose and l-alanine at different temperatures applying FTIR, NMR, EPR, and MALDI-ToF-MS. *Food Chem* 245:761–767. <https://doi.org/10.1016/j.foodchem.2017.11.115>
- Mohsin GF, Schmitt FJ, Kanzler C, Hoehl A, Hornemann A (2019) PCA-based identification and differentiation of FTIR data from model melanoidins with specific molecular compositions. *Food Chem* 281:106–113. <https://doi.org/10.1016/j.foodchem.2018.12.054>
- Cämmerer B, Kroh LW (1995) Investigation of the influence of reaction conditions on the elementary composition of melanoidins. *Food Chem* 53:55–59. [https://doi.org/10.1016/0308-8146\(95\)95786-6](https://doi.org/10.1016/0308-8146(95)95786-6)
- Kuntcheva MJ, Obretenov TD (1996) Isolation and characterization of melanoidins from beer. *Z Lebensm Unters Forch* 202:238–243. <https://doi.org/10.1007/BF01263547>
- Fogliano V, Morales FJ (2011) Estimation of dietary intake of melanoidins from coffee and bread. *Food Funct* 2(2):117–123. <https://doi.org/10.1039/c0fo00156b>
- Uddin MA, Yu H, Wang L, Naveed K, Haq F, Amin BU, Mehmood S, Nazir A, Xing Y, Shen D (2020) Recent progress in EPR study of spin labeled polymers and spin probed polymer systems. *J Polym Sci* 58:1924–1948. <https://doi.org/10.1002/pol.20200039>
- Renn PT, Sathe SK (1997) Effects of pH, temperature, and reactant molar ratio on L-leucine and D-glucose maillard

- browning reaction in an aqueous system. *J Agric Food Chem* 45(10):3782–3787. <https://doi.org/10.1021/jf9608231>
24. Shen Y, Tebben L, Chen G, Li Y (2018) Effect of amino acids on Maillard reaction product formation and total antioxidant capacity in white pan bread. *Int J Food Sci Technol* 54:1372–1380. <https://doi.org/10.1111/ijfs.14027>
 25. Kowalczyk D, Pitucha M (2019) Application of FTIR method for the assessment of immobilization of active substances in the matrix of biomedical materials. *Materials* 12(18):2972. <https://doi.org/10.3390/ma12182972>
 26. Rubinsztain Y, Yariv S, Ioselis P, Aizenshtat Z, Ikan R (1986) Characterization of melanoidins by IR spectroscopy—I. Galactose-glycine melanoidins. *Org Geochem* 9(3):117–125. [https://doi.org/10.1016/0146-6380\(86\)90101-4](https://doi.org/10.1016/0146-6380(86)90101-4)
 27. Rubinsztain Y, Yariv S, Ioselis P, Aizenshtat Z, Ikan R (1986) Characterization of melanoidins by IR spectroscopy—II. Melanoidins of galactose with arginine, isoleucine, lysine and valine. *Org Geochem* 9(6):371–374. [https://doi.org/10.1016/0146-6380\(86\)90118-X](https://doi.org/10.1016/0146-6380(86)90118-X)
 28. Guerrero-Pérez MO, Patience GS (2020) Experimental methods in chemical engineering: Fourier transform infrared spectroscopy—FTIR. *Can J Chem Eng* 98(1):25–33. <https://doi.org/10.1002/cjce.23664>
 29. Md Salim R, Asik J, Sarjadi MS (2021) Chemical functional groups of extractives, cellulose and lignin extracted from native *Leucaena leucocephala* bark. *Wood Sci Technol* 55:295–313. <https://doi.org/10.1007/s00226-020-01258-2>
 30. Woźniak M, Ratajczak I, Wojcieszak D, Waśkiewicz A, Szentner K, Przybył J, Borysiak S, Goliński P (2021) Chemical and structural characterization of maize stover fractions in aspect of its possible applications. *Materials* 14(6):1527. <https://doi.org/10.3390/ma14061527>
 31. Santos DI, Neiva Correia MJ, Mateus MM, Saraiva JA, Vicente AA, Moldão M (2019) Fourier transform infrared (FT-IR) spectroscopy as a possible rapid tool to evaluate abiotic stress effects on pineapple by-products. *Appl Sci* 9(19):4141. <https://doi.org/10.3390/app9194141>
 32. Ji Y, Yang X, Ji Z, Zhu L, Ma N, Chen D, Jia X, Tang J, Cao Y (2020) DFT-calculated IR spectrum amide I, II, and III band contributions of N-methylacetamide fine components. *ACS Omega* 5(15):8572–8578. <https://doi.org/10.1021/acsomega.9b04421>
 33. Kozłowicz K, Różyło R, Gładyszewska B, Matwijczuk A, Gładyszewski G, Chocyk D, Samborska K, Piekut J, Smolewska M (2020) Identification of sugars and phenolic compounds in honey powders with the use of GC-MS, FTIR spectroscopy, and X-ray diffraction. *Sci Rep* 10(1):16269. <https://doi.org/10.1038/s41598-020-73306-7>
 34. Baskaran S, Sathivelu M (2020) Application of Attenuated Total Reflection - Fourier Transform Infrared spectroscopy to characterize the degradation of littered multilayer food packaging plastics. *Vib Spectrosc* 109:103105. <https://doi.org/10.1016/j.vibspec.2020.103105>
 35. Awolu OO, Odoro JW, Adeloye JB, Lawal OM (2020) Physico-chemical evaluation and Fourier transform infrared spectroscopy characterization of quality protein maize starch subjected to different modifications. *J Food Sci* 85(10):3052–3060. <https://doi.org/10.1111/1750-3841.15391>
 36. Pawłowska-Góral K, Ramos P, Pilawa B, Kurzeja E (2013) Application of EPR spectroscopy to examination of the effect of sterilization process on free radicals in different herbs. *Food Biophys* 8(1):60–68. <https://doi.org/10.1007/s11483-013-9284-5>
 37. Hodge JE (1953) Dehydrated foods, chemistry of browning reactions in model systems. *J Agric Food Chem* 1(15):928–943. <https://doi.org/10.1021/jf60015a004>
 38. Kaufmann M, Krüger S, Mügge C, Kroh LW (2018) General acid/base catalysis of sugar anomerization. *Food Chem* 265:216–221. <https://doi.org/10.1016/j.foodchem.2018.05.101>
 39. Tressl R, Wondrak GT, Garbe L-A, Krüger R-P, Rewicki D (1998) Pentoses and hexoses as sources of new melanoidin-like maillard polymers. *J Agric Food Chem* 46(5):1765–1776. <https://doi.org/10.1021/jf970973r>
 40. Kanzler C, Haase PT (2020) Melanoidins formed by heterocyclic maillard reaction intermediates via aldol reaction and michael addition. *J Agric Food Chem* 68(1):332–339. <https://doi.org/10.1021/acs.jafc.9b06258>

Publisher's Note Springer Nature remains neutral with regard to jurisdictional claims in published maps and institutional affiliations.